N85-33519

THE DESIGN AND DEVELOPMENT OF A CONSTANT-SPEED SOLAR ARRAY DRIVE

Howard M. Jones and Neil Roger*

ABSTRACT

This paper describes the design and development of a constant-speed solar array drive system for use in high-power communications satellites. The relationship between continuity of motion in the solar array drive and spacecraft attitude disturbance is investigated. The selection of the system design based on the design requirements including spacecraft disturbance is discussed. The system comprises two main parts: the drive mechanism including small-angle stepper motor and reduction gearing and the control electronics including ministepping drive circuits, such that a very small output step size is achieved. Factors contributing to discontinuities in motion are identified and discussed. Test methods for measurement of very small amplitudes of discontinuity at low rotational rates are described to assist in the testing of similar mechanisms.

INTRODUCTION

The use of sun-pointing deployable solar arrays of increasing power levels on spacecraft for various applications has placed increased emphasis on the design and operational strategies of the solar array drives which maintain the sun-pointing attitude of the solar array while the spacecraft typically remains earth-pointing. As a result of increased solar array size and flexibility the potential to disturb spacecraft has increased dramatically. The use of a constant-speed drive as opposed to the more traditional intermittent or pulsed drive can improve this situation in two ways:

(a) The elimination of discontinuities in angular momentum between the solar array and the spacecraft results in reduced disturbance levels. This permits the use of smaller size or lower power consumption in the reaction or momentum wheels of the spacecraft pitch axis control loop, and/or less frequent momentum-dumping operations of the thrusters.

(b) The reduced energy levels in the dynamic coupling between the solar array and drive system leads to improved operating torque margins and eliminates potential problems of stalling and backdriving due to resonant array dynamics. This phenomenon occurred on-orbit in a large communications satellite recently, resulting in forcible back-stepping of the system while a step forward had been commanded.

However, because the required rate of rotation is very low (i.e., 1 revolution per day for geosynchronous spacecraft), the maintenance of constant speed within limits, expressed as a proportion of the nominal speed, is a difficult proposition. The fundamental problem is therefore one of achieving the necessary continuity of motion in the solar array drive system without leading to excessive mechanical and electrical complexity with the resulting penalties in reliability, cost and mass.

*Spar Aerospace Limited, Toronto, Canada

REQUIREMENTS

The continuity of motion requirements for the solar array drive system are derived from analysis of the relationship between speed variations in the drive system and spacecraft disturbance using computer simulations of the drive system, solar array, spacecraft body with flexible appendages and the spacecraft pitch axis control loop.

A typical spacecraft configuration is shown in Figure 1 corresponding to a high-power geosynchronous communications application. Data for the spacecraft, its' flexible appendages and attitude control system parameters are summarized in Table I.

From the computer simulations it was determined that both the amplitude and frequency of speed variations in the solar array drive were important. The approaches used and the continuity of motion achieved are discussed in the Design and Analysis section below.

The spacecraft disturbance and other relevant drive system requirements are presented in Table II.

DESIGN AND ANALYSIS

The design and analysis proceeded in three stages:

(a) Analysis of the relationship between continuity of motion in the solar array drive and spacecraft disturbance using computer simulations of the drive system, solar array, spacecraft body with flexible appendages and the pitch-axis control loop.

(b) Evaluation and trade-off of various drive system concepts to determine which would best achieve the required continuity of motion requirements in terms of reliability, cost and mass.

(c) Further design and analysis of the selected concept.

Drive System Concepts and Trade-off

The concepts considered fell into one of the two main categories:

- Open-loop stepper and synchronous systems.
- Closed-loop brushless DC systems using rate or position sensor feedback (in addition to commutation feedback).

A variety of gear ratios was also considered for each category.

It was found that because the nominal rotation rate is very low (1 revolution per day) the fluctuations in rate, expressed as a proportion of the nominal, are very small and hence difficult to detect and to control for the closed-loop systems. Therefore the open-loop stepper or synchronous approach was selected due to its simplicity. The system block diagram for the open-loop geared stepper concept is illustrated in Figure 2.

The other major trade-off area involved selection of the optimum combination of techniques for reducing output step size for the stepper or synchronous concepts. The following methods are available:

(a) Motor with small prime step angle.
(b) Electronic step division (mini-stepping).
(c) Reduction gearing.

Gear reductions are selected for other reasons including motor torque amplification (reduces system size and weight) and backdrive characteristics (e.g., low backdrive efficiency reduces susceptibility to solar array dynamic torques). The selected concept uses a conventional 1.8° stepper motor with 64-level mini-stepping and 288:1 reduction gearing to achieve a theoretical output step size of 0.0001°. This step size is so low and the associated stepping frequency of 42 Hz so high, that significant interaction with the solar array and the spacecraft pitch axis control loop are avoided. The lamination shapes for a hybrid stepper motor with 1.8° prime step angle are illustrated in Figure 3, with the associated electrical schematic and sinusoidal ministep drive sequence. The schematic of the ministep electronics is shown in Figure 4. A cutaway illustration of the 288:1 reduction gearing is presented in Figure 5. The second stage of the reduction gearing is a regenerative planetary set which is non-backdriveable. This set functions in a similar fashion to the harmonic drive except that the nutating flexible spline of the later has been replaced by the more robust planet gears, which can withstand much higher backdrive loads. More detailed information on the gears is presented in Table III.

Factors Affecting Continuity of Motion

As described above the selected drive system provides a theoretical output step size of 0.0001° and a stepping frequency of 42 Hz. In practice the drive mechanism will be part of a solar array drive assembly which includes bearings and slip rings mounted on the main shaft. It has been predicted that the achievable continuity of motion at the output is limited by stick-slip effects in the system.

Due to the compliance of the drive train and the slow, synchronous speed of the motor there is a finite rate of drive torque build-up in the main shaft. Therefore when the system is started from zero rate it takes a finite time for the drive torque in the shaft to exceed the static friction due to the slip rings and bearings. Let this time be called T_1. When the breakout torque is exceeded the shaft accelerates to a speed higher than the nominal rate under the action of the "wind-up" torque in the drive train. As the "wind-up" torque falls below the friction torque the shaft speed decreases until it is caught by static friction. Let this time interval (of relative motion at the slip rings) be called T_2. The process is then repeated and is illustrated in Figure 6A.

The phenomenon could only be completely eliminated by the total elimination of friction or by the addition of viscous or damping friction into the system. However, the problems associated with the stick slip effects can be alleviated by controlling the times T_1 and T_2 and hence the amplitudes of discontinuities in the main shaft rotation. The following parameters were found to affect T_1 and T_2:

(a) Drive system stiffness.
(b) Absolute levels of static and dynamic friction.
(c) Relative levels of static and dynamic friction.
(d) Level of viscous friction in the system.
(e) Solar array dynamics.

The ratio of static to dynamic friction in the slip rings is determined by the properties of the materials used and is not amenable to manipulation. The solar array dynamics are not generally subject to alteration for this purpose while the addition of sufficient viscous friction into the system at these low rates would not be practical. This generally leaves the drive system stiffness and the absolute friction levels under the control of the solar array drive designer. Increasing the drive system stiffness and reducing the slip ring friction levels will decrease the period (T_1 + T_2) and hence the amplitude of the rate discontinuities. A parametric analysis using the computer simulations mentioned earlier was conducted to determine acceptable combinations of stiffness and friction. The predicted effects of various combinations of slip ring friction and drive system stiffness on continuity of motion are illustrated in Figure 6B. This indicates that to maintain an output step size in the same range as the theoretical value, say 0.0003° maximum, the slip ring dynamic friction should be limited to 1.3 Nm and the drive system stiffness at the main shaft should be above 150,000 Nm/radian. While this stiffness is not generally difficult to achieve in a solar array drive mechanism, the limit of 1.3 Nm sliding friction presents a challenge for the larger slip ring assemblies, particularly those of the disc configuration due to the larger diameter of the rings.

TESTING

An engineering model drive system has been built including the ministepping electronics. The test program in progress includes:

(a) Ambient performance tests (torque-speed, etc.).
(b) Environmental testing (vibration and thermal vacuum).
(c) Continuity of motion (systems dynamics).

The ambient performance and environmental testing involve conventional procedures and techniques and need not be discussed further. However, the system dynamics test includes a novel approach for measuring continuity of motion at the output under various operating conditions and is described below.

The purpose of the System Dynamics test is to determine the dynamic characteristics of the Solar Array Drive Assembly (SADA) under various operational conditions. The operational conditions to be represented (or accounted for) are:

(a) Solar array dynamics.
(b) Slip ring friction.
(c) Rotational rates (for sun acquisition and sun-tracking modes).

The system dynamics test rig illustrated in Figure 7 was designed and fabricated to represent the appropriate solar array torsional modes and the slip ring friction. The inertia and stiffness of the simulated solar array and the friction of the simulated slip ring can be adjusted to represent various operational conditions of interest. The drive system can be commanded to run at a variety of rotational rates including those corresponding to typical sun-acquisition and sun-tracking modes for geosynchronous and low-earth orbits.

The main indicator of system performance is the continuity of motion achieved at the SADA output. This parameter readily indicates any problems in the system such as temporary stalling, excessive stick-slip effects or solar array excitation. The relationship between continuity of motion and levels of spacecraft disturbance and solar array excitation was discussed above. Since the predicted discontinuities in the SADA output motion are low, the question of measurement techniques is important.

Dynamics analyses discussed above indicated that the expected discontinuities in rotational rate have amplitudes of 0.0001 to 0.0007 degree and periods of 23 to 170 milliseconds (frequencies of 4-60 Hz approximately).

Two alternatives were considered for determining these discontinuities:

(a) Position or rate sensing.
(b) Acceleration sensing.

Position or Rate Sensing

The predicted amplitudes of the discontinuities are so low that extremely high resolution position sensing is required to measure them to, say, 0.00005 degree. The only feasible techniques identified were either an inductosyn resolver or an optical encoder-resolver, both with digital interpolation electronics. The required resolution is equivalent to a 23-bit encoder. The sensor generates position versus time data from which the velocity profile of the drive output can be derived.

Several drawbacks were identified with this approach:

- o The sensor is a special, long-lead and expensive device.
- o The sensor would have to be mounted extremely accurately to the SADA/array interface or would require its own precision bearing system with flexible coupling to the SADA shaft.
- o The significant rigid inertia of the sensor rotor would affect the dynamics.

Acceleration Sensing

To overcome the disadvantages associated with the use of the high-resolution position sensor, an alternative approach involving an accelerometer to sense the discontinuities was developed. In this case a high-resolution linear accelerometer is mounted on a stiff, light moment arm attached to the output shaft. The accelerations due to the discontinuities in motion can then be detected and integrated to obtain the velocity profile as shown in Figure. 8.

The limited bandwidth of the accelerometer is predicted to result in some truncation of the acceleration spikes at initiation and termination of each discontinuity when these occur at the higher end of the frequency range identified above, i.e., 20-60 Hz. This, in turn, will result in errors in the velocity profiles derived by integration of the accelerometer output and is illustrated in Figure 8. However, this is not considered serious because:

(a) The errors only become significant at frequencies corresponding to performance considerably better than the continuity of motion requirements derived above.

(b) The velocities can be corrected to some extent by reference to the average orbital rate.

CONCLUSIONS

A constant-speed solar array drive has been developed which offers significant improvements in the levels of spacecraft disturbance and solar array excitation compared with more traditional intermittent and stepper drives. The required continuity of motion has been achieved with an open-loop system using an optimum combination of small prime step angle in the motor, electronic step division, and reduction gearing. This largely preserves the simplicity associated with open-loop stepper drives. The two-stage regenerative planetary gearset is an interesting variation on the harmonic drive concept.

An engineering model drive system including the ministepping electronics has been fabricated and is currently undergoing a series of tests. Of particular interest is the method of measuring the achieved continuity of motion at the output under various operating conditions. A novel approach was adopted involving a sensitive linear accelerometer mounted on a stiff, light moment arm attached to the output shaft of the drive system. The accelerometer signal can be processed in a variety of ways to derive the angular velocity profile, frequency spectrum, etc.

The design and test techniques described in this paper are applicable to other low-speed mechanisms such as robot arm joints and pointing drives for large antennae.

ACKNOWLEDGEMENTS

This paper describes work performed under the sponsorship and technical direction of the International Telecommunications Satellite Organization (INTELSAT). Any views expressed are not necessarily those of INTELSAT. The authors would like to thank Mr. W. Alsbach of INTELSAT for his valuable support and advice.

The prior support of the Canadian Government Department of Communications/CRC for developing various aspects of solar array drive technology is also gratefully acknowledged.

TABLE I SPACECRAFT DATA

A. MASS PROPERTIES		
MASS	:	6,350 kg
MoI - ROLL	:	52,000 kgm^2
- PITCH	:	32,000 kgm^2
- YAW	:	46,000 kgm^2
B. FREE-FREE MODES OF SPACECRAFT AND ANTENNA		
MODE NO.	AXIS	FREQUENCY
7	ROLL-YAW	0.167 Hz
8	PITCH	0.176 Hz
9	ROLL-YAW	0.243 Hz
C. SOLAR ARRAY FIXED-BASE TORSIONAL (PITCH-AXIS) MODES		
MODE NO.	FREQUENCY	MODAL INERTIA
1	0.0984 Hz	113 Kgm^2
3	0.1487 Hz	80 Kgm^2
D. ACS PITCH AXIS		
POINTING REQUIREMENTS	:	± 0.03°
MOMENTUM CAPACITY	:	± 10 Nms
SATURATION TORQUE	:	0.1 Nm
NATURAL PERIODS	:	13s AND 125s

TABLE II DRIVE SYSTEM DESIGN REQUIREMENTS

DRIVE TORQUE - (3 cx WORST-CASE RESISTING TORQUES)	16 Nm, MINIMUM
SOLAR ARRAY ORIENTATION - POINTING ACCURACY - DEVIATION BETWEEN NAND S WINGS - SUN-TRACKING RATE - SUN-ACQUISITION RATE	± 2.0° 0.2° 1 REVOLUTION PER DAY 0.27° PER SECOND
INDUCED SPACECRAFT DISTURBANCE (PITCH-AXIS) - POINTING ERROR - REACTION WHEEL TORQUE - REACTION WHEEL MOMENTUM CHANGE	0.03°, MAXIMUM 0.1 Nm, MAXIMUM 1.0 Nms, MAXIMUM*
* 10% OF TOTAL REACTION WHEEL CAPACITY FROM TABLE I	

TABLE III GEAR DATA

A. FIRST STAGE : EXTERNAL SPUR SET	
NUMBER OF TEETH ON PINION NUMBER OF TEETH ON GEAR RATIO =200 / 34	: 34 : 200 = 5.88
MODULE (DIAMETRAL PITCH) PRESSURE ANGLE EFFICIENCY, NOMINAL	: 1.06 mm (24) : 20° : 98%
B. SECOND STAGE : REGENERATIVE PLANETARY SET	
NUMBER OF TEETH ON PLANET NUMBER OF TEETH ON FIXED RING NUMBER OF TEETH ON ROTATING RING RATIO = $\frac{98 \times 27}{(98 \times 27) - (96 \times 27)}$	: 27 : 96 : 98 = 49
MODULE (DIAMENTRAL PITCH) PRESSURE ANGLE EFFICIENCY, NOMINAL	: 0.94 mm (26.889) : 22.5° : 30%

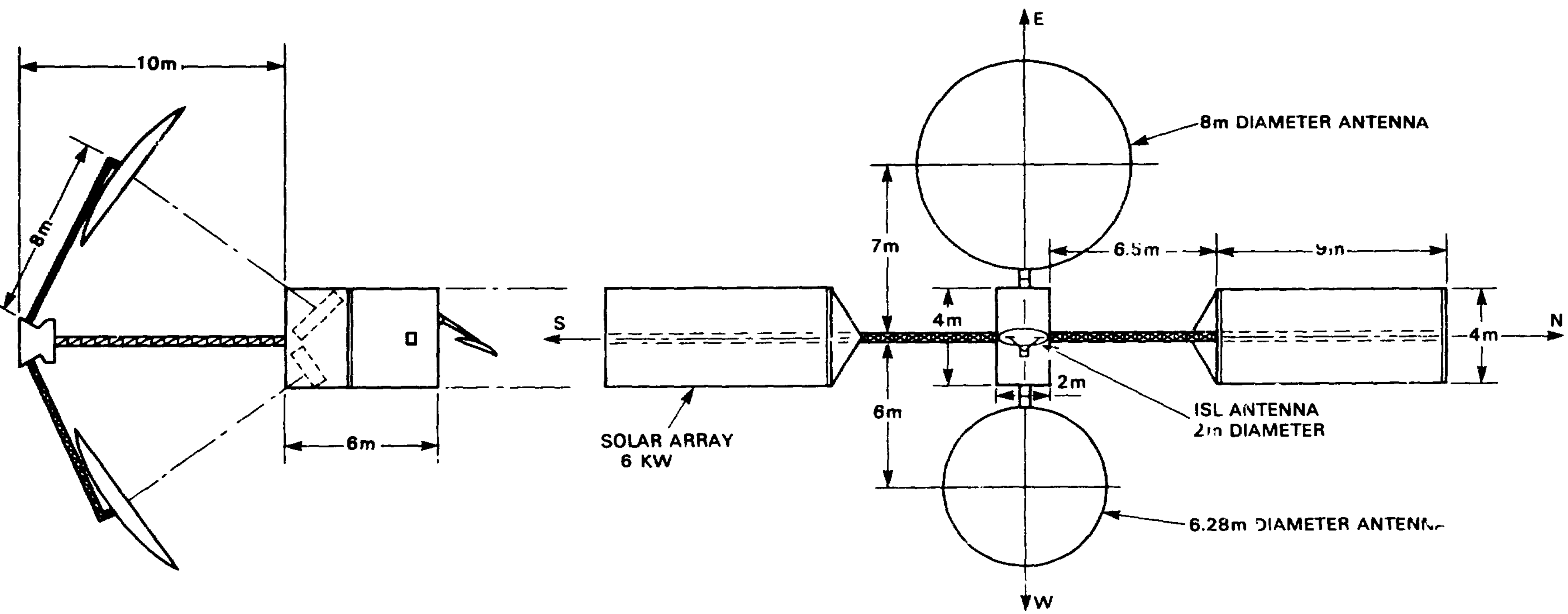

FIGURE 1 SPACECRAFT CONFIGURATION

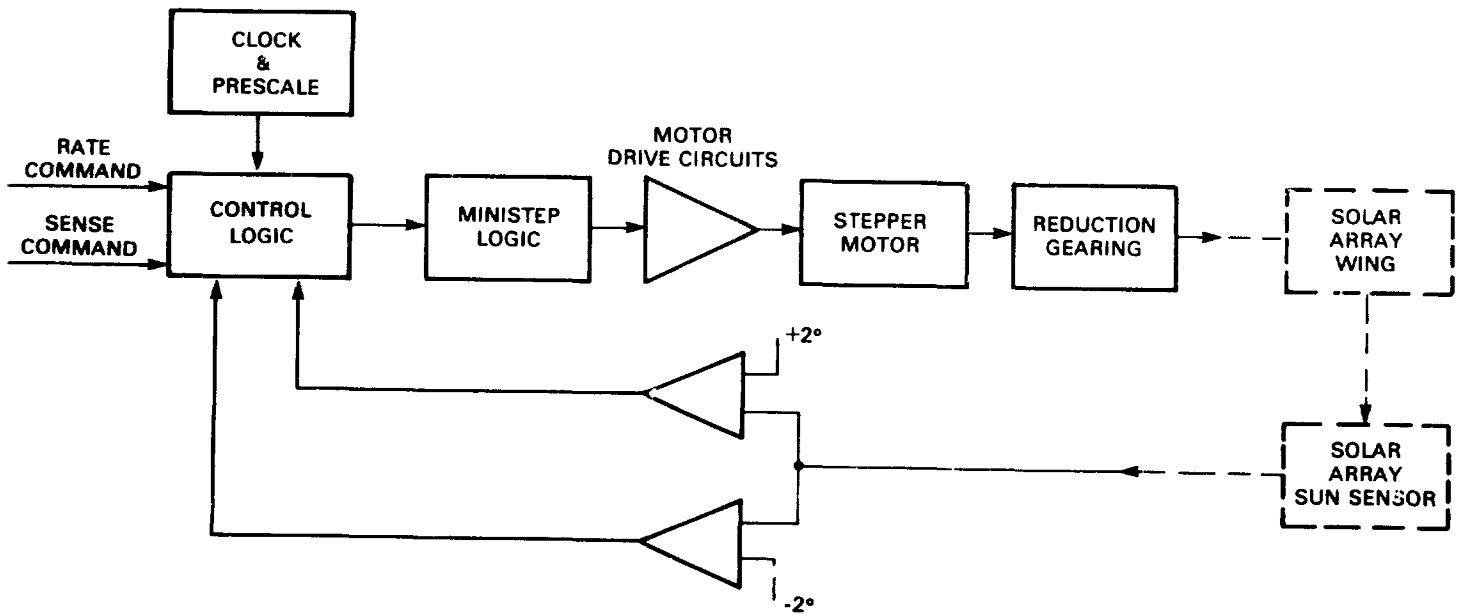

FIGURE 2 DRIVE SYSTEM BLOCK DIAGRAM

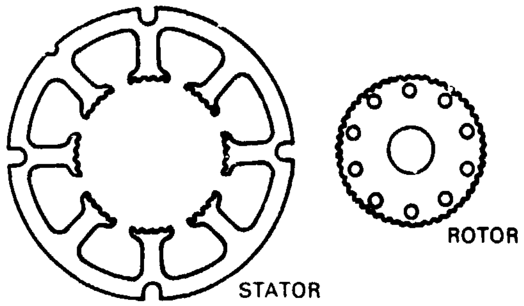

MOTOR LAMINATIONS SHAPES

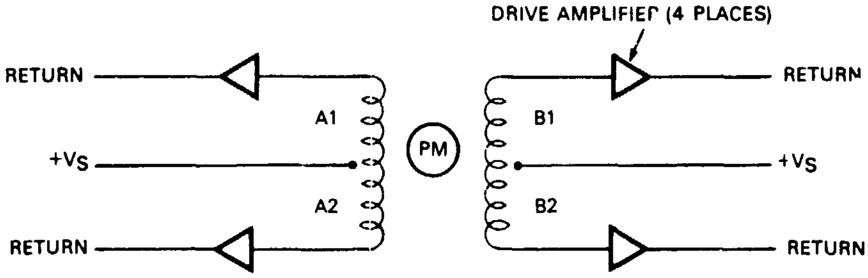

MOTOR AND DRIVER SCHEMATIC

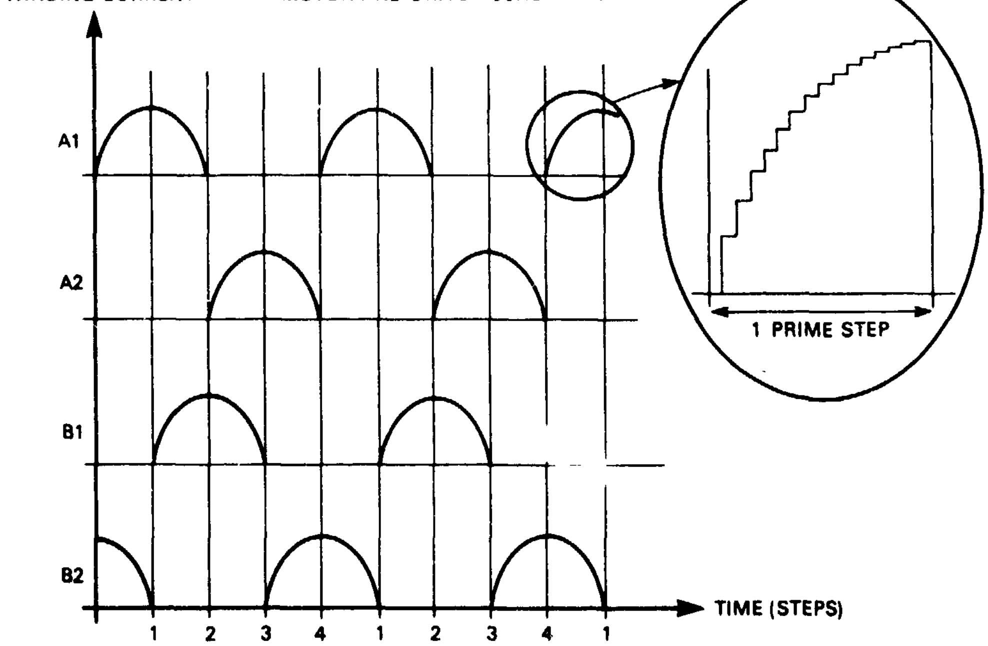

SINUSOIDAL MINISTEP DRIVE SEQUENCE

FIGURE 3 MOTOR DETAILS AND DRIVE SEQUENCE

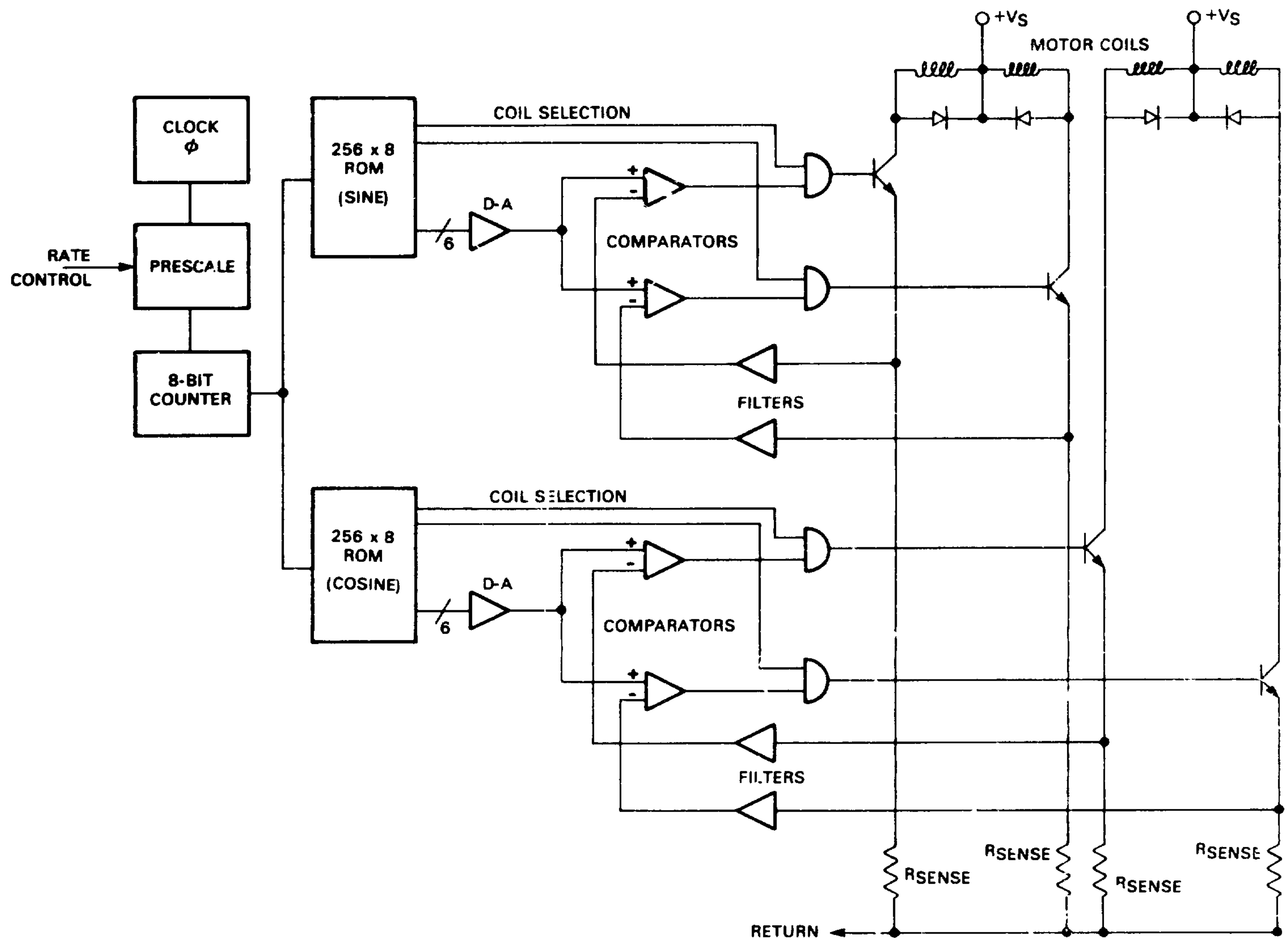

FIGURE 4 SCHEMATIC OF MINISTEPPING ELECTRONICS

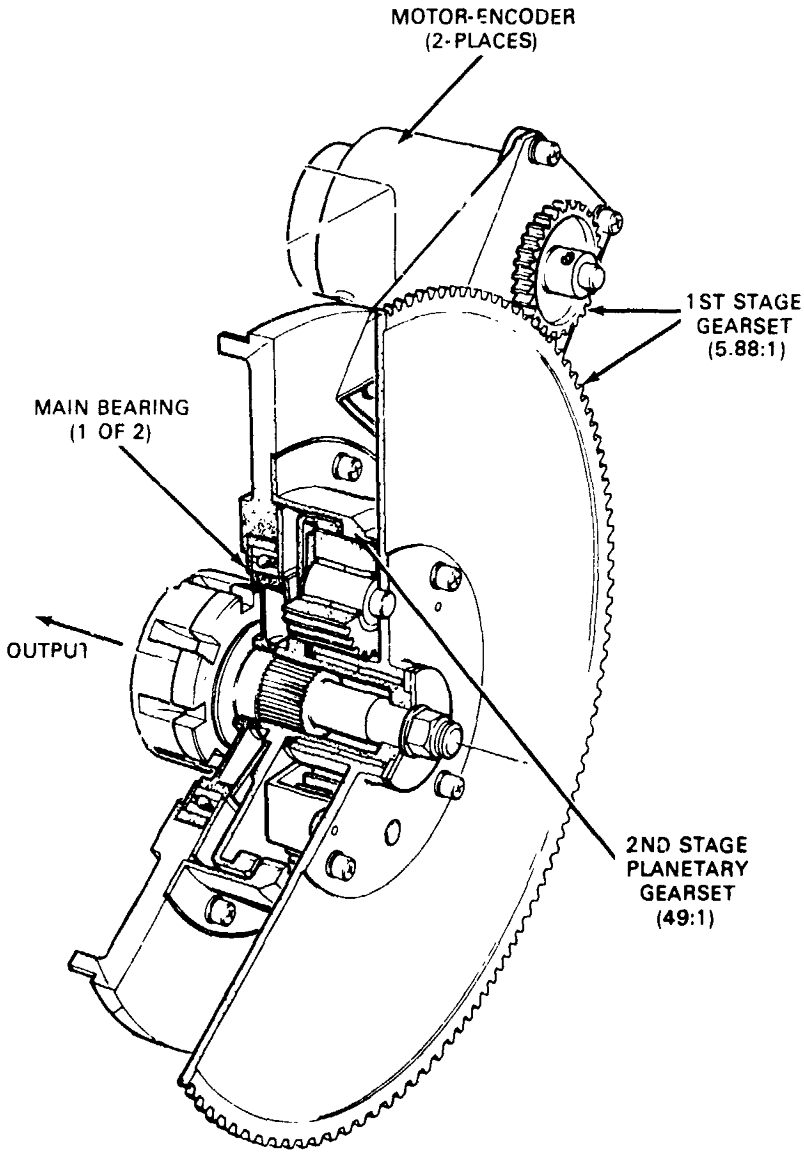

FIGURE 5 CUTAWAY ILLUSTRATION OF REDUCTION GEARING

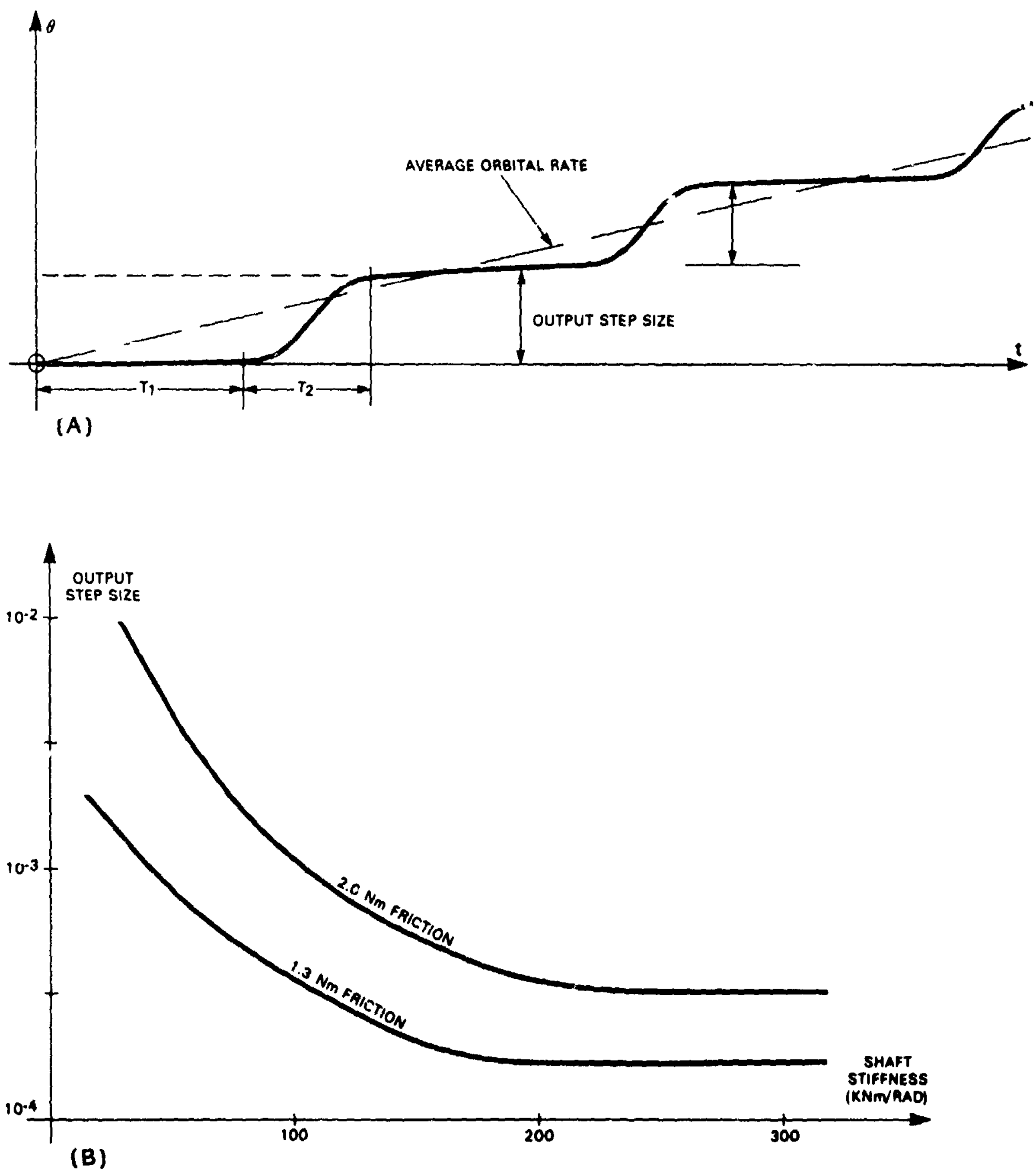

FIGURE 6 STICK-SLIP MOTION AND EFFECTS OF FRICTION AND STIFFNESS

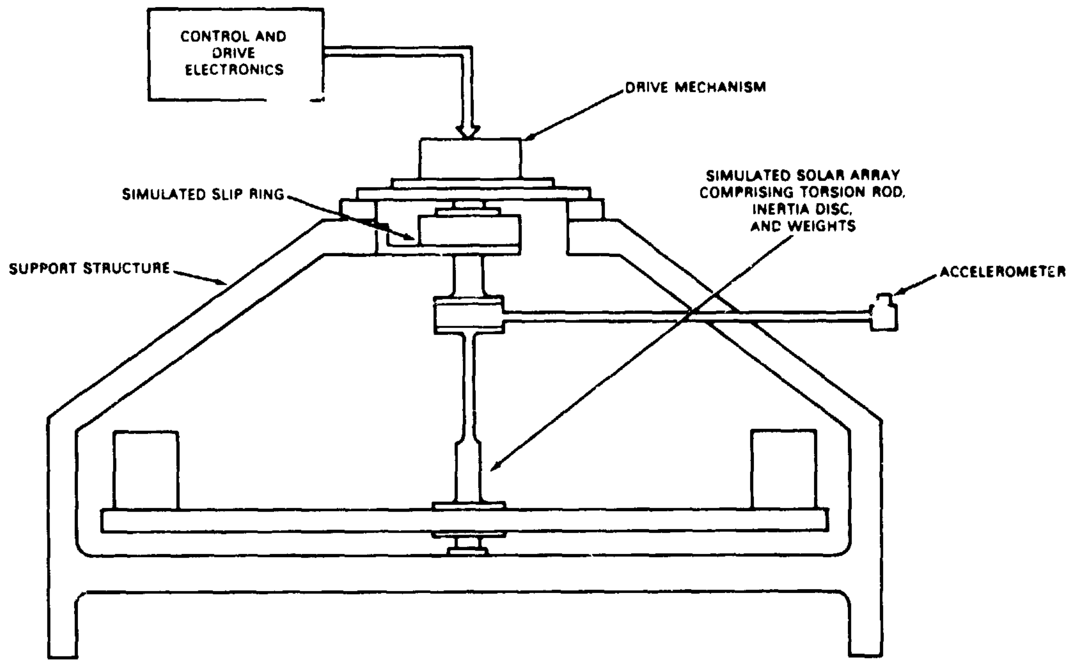

FIGURE 7 SYSTEM DYNAMICS TEST RIG

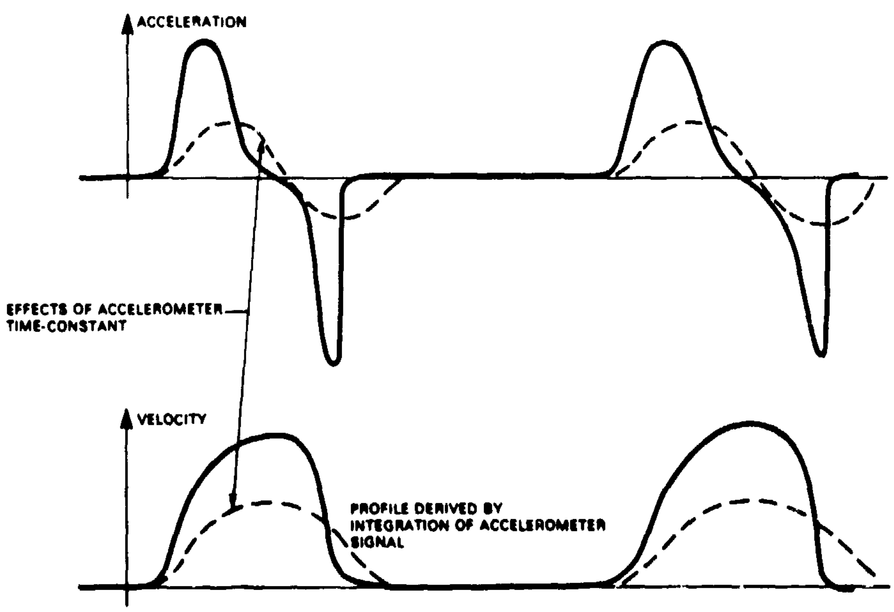

FIGURE 8 DETERMINATION OF CONTINUITY OF MOTION